

Synthesis and characterization of AC-CdO-TiO₂ nanocomposite recyclable and multi-application study.

Marimuthu G^{1*}, Prithivirajan B², Jebastin Sonia Jas M^{2,3}

¹Department of Chemistry, Swami Dayananda College of Arts and Science, Manjakkudi, Tiruvarur District, Tamil Nadu, India

²Research and Development Centre, Bharathiar University, Coimbatore, India

³Department of Chemistry, IFET College of Engineering, Villupuram, India

Abstract

The synthesis of AC-CdO-TiO₂ nanocomposite material has been successfully achieved by precipitation method and sonication technique. High photocatalytic activity of AC-CdO-TiO₂ nanocomposite material used Reactive Black 5 (RB 5) under UV-light irradiation and that of TiO₂; the nanocomposite material was characterized by High-Resolution Scanning Electron Microscopy (HR-SEM) with Elementary Dispersive X-ray (EDX), High-Resolution Transmission Electron Microscopy (HR-TEM), XRD analysis, Photoluminescence spectroscopy (PL) and UV-Vis DRS analysis. This nanocomposite material obtained by photodegradation of RB 5 dye at various parameters is reported. The reaction of this nanocomposite material was found to be stable and reusable. The antibacterial activity of prepared material was investigated against Gram negative and positive bacterial strains and through their electrochemical activity.

Keywords: RB 5 dye, Catalyst, Antibacterial activity, Electrochemical activity.

Accepted on August 9, 2018

Introduction

Dye molecules are used for textile industry in manufacturing production, clothing, wastewater from printing and photodegradation materials [1-5]. Semiconductor oxide (CdO, TiO₂, ZnO and SnO₂), is an exceptional photocatalyst, medicine and sensing element for optoelectronic applications [6-10].

Titania semiconductors are used in photocatalyst, paint industries, paper, and plastics industries due to the presence of excellent semiconductor oxide [11]. Two or more semiconductors with appropriate band energy levels is an improved way to increase the photocatalytic activity of the semiconductor because of the useful separation of photogenerated electron-hole pairs and interfacial charge transfer efficiency [12-14]. Such semiconductor oxides have been considered to hold an effective chemical, physical and photocatalytic properties [15,16]. Recently complex semiconductor oxides have been reported to show similar properties [17-22]. Activated carbon is a brilliant adsorbent of waste water pollutants, due to the following reasons (i) activated carbon adsorb the dye and release it on surface of the photocatalyst (ii) degradation by oxidation [23-25]. Activated carbon-loaded semiconductor oxide undergoes high photodegradation [26-28].

The nanocomposite material was characterized by high-resolution scanning electron microscopy (HR-SEM) with elementary dispersive X-ray (EDX), high-resolution transmission electron microscopy (HR-TEM), XRD analysis; photoluminescence spectroscopy (PL) and UV-Vis DRS. This nanocomposite material can photodegrade RB 5 dye at various parameters under the UV-light irradiation at 365 nm.

The mineralization of dyes is confirmed by chemical oxygen demand measurements. An achievable mechanism is proposed for higher activity of AC-CdO-TiO₂ that of TiO₂ nanocomposite material. Reaction of this nanocomposite material was found to be stable and reusable. AC-CdO-TiO₂ nanocomposite material showed highest antibacterial activity and electrochemical activity compared to that of TiO₂ nanocomposite material.

Experimental Section

Materials

Cadmium acetate dehydrates, tetra isopropyl orthotitanate (C₁₂H₂₈O₄Ti), reactive black 5 (RB 5) dye and activated carbon (AC), citric acid, NH₄OH were used as received. Coumarin (1 mM of 4-hydroxycoumarin) is a chemical of Sigma Aldrich and used as such. The ethanol and aqueous solution was obtained using double distilled water. All

glasswares were cleaned with acid followed by thorough washing with distilled water.

Preparation of AC-CdO-TiO₂ nanocomposite material by precipitation method

AC-CdO-SnO₂ nanocomposite material was synthesized by precipitation method. Initially cadmium acetate dihydrate (0.4 M) was dissolved in anhydrous ethanol solution in beaker A. 0.4 M citric acid and tetra isopropyl orthotitanate in ethanol is taken as another solution in beaker B and activated carbon (AC) was dissolved in anhydrous ethanol solution in beaker C, the solution in A and solution in C are added to solution in beaker B and stirred well. To these 2 drops of NH₄OH is added at room temperature under vigorous stirring until the precipitate was formed. The obtained precipitate was washed with water and ethanol. Then the precipitate was collected and dried in oven at 100°C for 12 h. The resulting powder was finally calcinated at 500°C at 4 h (Figure 1).

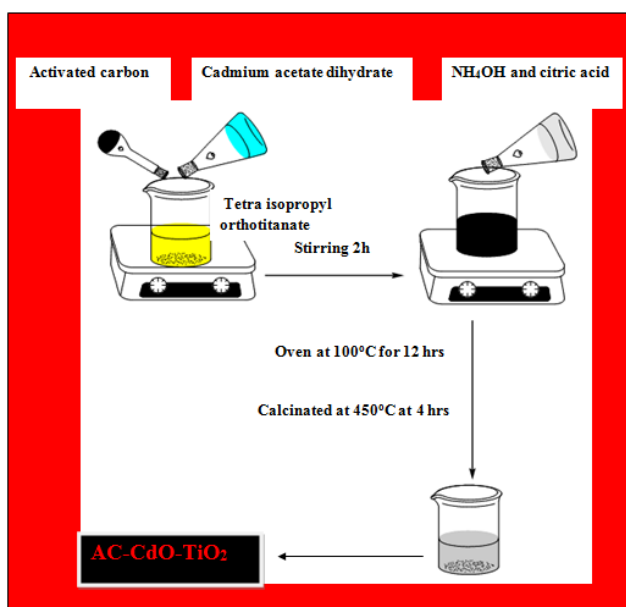


Figure 1. Preparation of AC- CdO-SnO₂ nanocomposite material stirred.

Characterization

Ultraviolet and visible (UV-vis) absorbance spectra were measured over a range of 800-200 nm with a Shimadzu UV-1650PC recording spectrometer using a quartz cell with 10 mm optical path length. High resolution scanning electron microscopy (HR-SEM) as well as elementary dispersive X-ray (EDX) evaluation experiments was performed on a FEI Quanta FEG 200 instrument with EDX analyzer facility at 25°C. The nanoparticles' size and structure verifications were done by transmission electron microscopy (HR-TEM) making use of PHILIPS CM200. Each spectrum was recorded with an acquisition time of 18 s. XRD spectrum was recorded on the X'PERT PRO model X-ray diffractometer from pan analytical instruments operated at a voltage of 40 kV and also a current of 30 mA with Cu K α radiation. Photoluminescence (PL) spectra

at a room temperature were recorded using a Perkin-Elmer LS 55 fluorescence spectrometer. UV spectral measurements were done using a Hitachi-U-2001 spectrometer. Ultraviolet and visible (UV-vis) absorbance spectra were measured over a range of 800-200 nm with a Shimadzu UV-1650PC recording spectrometer using a quartz cell with 10 mm of optical path length. The antibacterial activity was studied by disc diffusion method; the test compound was dissolved in DMSO (200 mg/ml) for about half an hour. Commercially available drug disc, ciprofloxacin (10 mg/disc) was used as positive reference standard and cyclic voltammetry (CV) measurements were carried out using CHI 60 AC electrochemical analyzer (CHI Instruments Inc. USA). The Photovoltaic properties of the material was characterized by recording the photo current voltage (I-V) curve under illumination of A.M.1.5 (100 MW/cm²).

Photocatalysis

The photocatalytic activities of the photocatalysts AC-CdO-SnO₂ nanocomposite material were evaluated by the photodegradation of dye. The light source was UV lamp at 365 nm. The reaction was carried out at ambient temperature (303 K). Aqueous suspensions of dye (40 ml, 1 \times 10⁻⁴ M) and 0.080 g of photocatalyst were loaded in reaction tube of 50 ml capacity with a prior 40 min in the irradiation, the suspension was magnetically stirred in dark to ensure the establishment of an adsorption or desorption equilibrium. The suspension was kept under constant air-equilibrated condition. At the intervals of given irradiation time. The suspension was measured spectrophotometrically at max=595 nm (RB 5) within the theory to Beer-Lambert law limit.

Results and Discussion

HR-SEM with EDX analysis

The HR-SEM image of AC-CdO-TiO₂ nanocomposite material is shown in Figure 2a. The particles are in the form of aggregates, uniformly distributed in various sizes and have a morphological structure of nanoflakes. The AC-CdO-TiO₂ nanocomposite material maintained at a high calcination temperature for 4 h and presented in RB 5 dye was shown to have highly photocatalytic activity. Figure 2b shows EDX analysis which confirms that only Ti, Cd, C and O are present in AC-CdO-TiO₂ nanocomposite material.

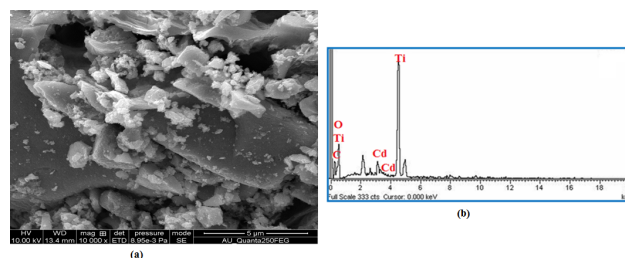


Figure 2. HR-SEM image of (a) AC-CdO-TiO₂ nanocomposite material and (b) EDX analysis.

HR-TEM analysis

The high-resolution transmission electron microscope (HR-TEM) measurements of AC-CdO-TiO₂ nanocomposite material are shown in Figure 3a. It is established that the presence of particles are depicted from the HR-TEM micrographs of the mixed nanoparticles at 20 nm as nanospherical chain shaped structure. In Figure 3b, the selected area of electron diffraction (SAED) pattern shows bright diffraction rings corresponding to polycrystalline nature.

This revealed that the high resolution TEM images (HR-TEM) and selected area diffraction pattern (SADP) of AC-CdO-TiO₂ nanocomposite material. It was seen that the crystal grain size, crystalline volume, and crystallinity reduced as the doping ratio increased in accordance with the XRD results. The tiny spherical particles with a high surface area make superior contact area with microbe. Figure 3c represented an image profile and Figure 3d shows the particle size distribution by selected particle area (0.261 nm) as highlighted in Figure 3a.

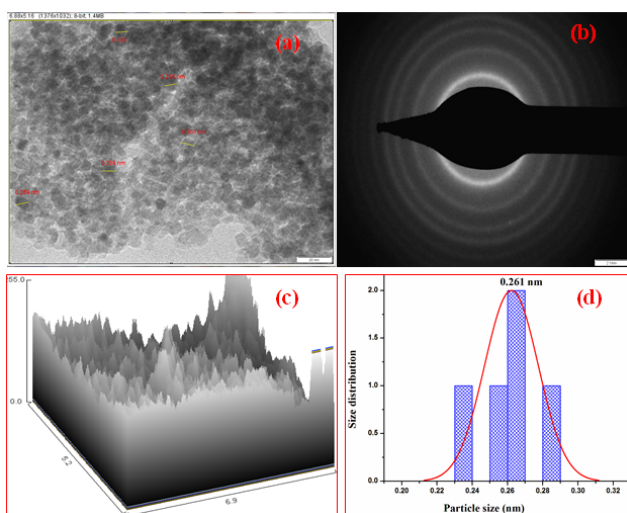


Figure 3. HR-TEM analysis of AC-CdO-TiO₂ nanocomposite material (a) TEM Image (b) SAED pattern (c) Surface plot and (d) Particle size in selected area highlighted in (a).

XRD analysis

The XRD spectra of TiO₂ and AC-Cd-TiO₂ nanocomposite material were shown in Figures 4a and 4b respectively. According to the crystal structure spectra, the well-defined peaks typical of TiO₂ were clearly noticed. This is in compliance with the reports of the norms of the Joint Committee on Powder Diffraction Standard JCPDS card no. 21-1272. Samples gave six distinctive TiO₂ peaks at 25, 29.91, 38.0, 47.87, 56.92, 64.5 and 74.74 as shown in Figure 4a with the diffractions of the TiO₂ (1 0 1), (0 0 4), (2 0 0), (1 0 5) and (2 0 4) crystal planes (anatase TiO₂).

The XRD spectrum of AC-CdO-TiO₂ nanocomposite material is shown in Figure 4. In the Figure 4b the distinctive peaks at 25, 29.32, 34.5, 47.87, 56.94 64 and 70.62, 78 were represented respectively. X-ray diffraction pattern was calculated using the Debye-Scherrer formula, $L=0.89 \lambda/\beta \text{ Cos } \theta$

where L is the crystalline size (nm), λ is the wavelength (nm), β is the full width at half maximum intensity (FWHM-in radian), and θ is the Bragg diffraction angle (°). The average crystalline sizes of the AC-CdO-TiO₂ nanocomposite material products were calculated to be about 21 nm.

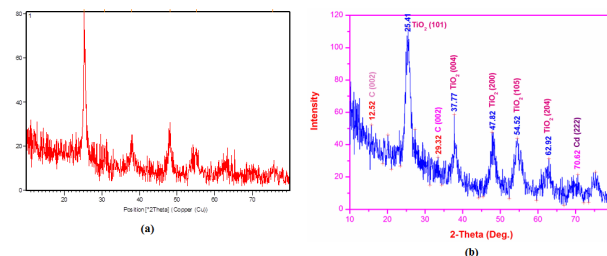


Figure 4. XRD pattern of (a) TiO₂ and (b) AC-CdO-TiO₂ nanocomposite material.

PL analysis

PL spectra of prepared TiO₂ and AC-CdO-TiO₂ nanocomposite material were shown in Figures 5a and 5b respectively. As the photoluminescence occurs due to electron-hole recombination, its intensity is directly proportional to the rate of electron-hole recombination and is directly proportional to the rate of electron-hole recombination. The prepared TiO₂ gave two emissions at 425 and 480 nm. The prepared AC-CdO with TiO₂ does not shift the emission of TiO₂ but the intensity of PL emission is less when compared to TiO₂ nanocomposite material. The improved near band edge emission (NBE) of pure TiO₂ shows better crystallinity, whereas the slight decrease of NBE in the AC-CdO with TiO₂ indicates the increase of intrinsic defect and is the reason for the decrease of near band edge emission present increases photocatalytic activity, this is because of suppression of recombination of electron-hole pairs by which better photocatalytic activity.

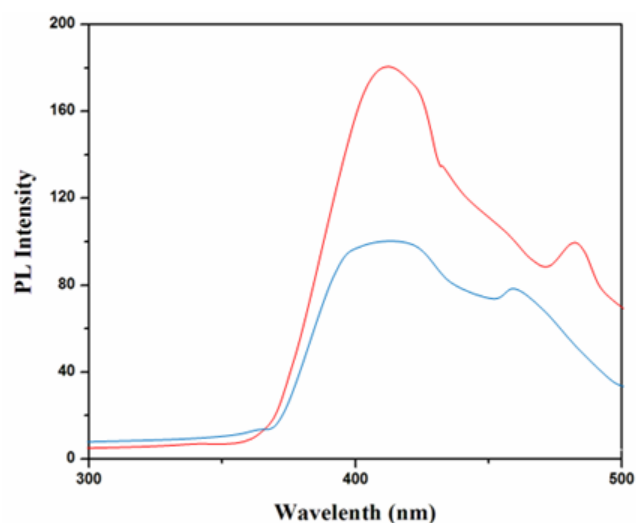


Figure 5. PL analysis (a) TiO₂ and (b) AC-CdO-TiO₂ nanocomposite material.

UV-vis DRS spectrum

UV-Vis-DRS (diffuse reflectance spectra) analysis of TiO₂ and AC-CdO-TiO₂ nanocomposite material was displayed in Figure 6. The bio-synthesis AC-CdO-TiO₂ nanocomposite material shows increased absorption in both UV and visible region than that of TiO₂ nanocomposite material and can be used as a UV and visible light active semiconductor photocatalytic nanocomposite material. The UV-Vis spectra were transformed to the Kubelka-Munk function $F(R)$ to separate the extent of light absorption from scattering. The band gap energy is obtained from the plot of the modified Kubelka-Munk function $(F(R)E)^{1/2}$ versus the energy of the absorbed light E by the Equation 1.

$$(1-R)^{1/2}$$

$$(F(R)E)^{1/2} = (X h \nu) \rightarrow (1)$$

2R

The final result indicates band gap energy of 3.4 eV and 3.0 eV corresponding to the chemical synthesized TiO₂ and AC-CdO-TiO₂ nanocomposite material. The lower band gap energy supports for superior photocatalytic activity [29].

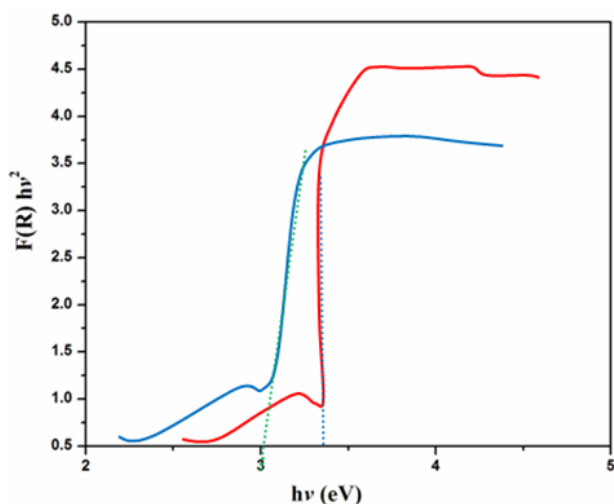


Figure 6. UV-Vis DRS analysis of (a) TiO₂ (b) AC-CdO-TiO₂ nanocomposite material.

Photodegradation of RB 5 dye

Primary analysis (Photodegradation of RB 5 dye with artificial UV-light): The pH analysis in photodegradation of RB 5 dye compared to fast dye was investigated in the pH range 3, 7, 9 and 11 and the results were reported. It was observed that the degradation increases with an increase in pH up to 7 and then decreases.

The photodegradation of RB 5 dye in aqueous medium in the presence of catalyst and the atmospheric air were studied using multi lamp photoreactor with mercury UV lamps at wavelength 365 nm. The initial dye concentration was 1×10^{-4} M and the pH of dye is neutral (pH=7). It was shown to be in dark colour. After photodegradation, the colour changes at irradiation time 40 min as shown in Figure 7. The reaction time affords the

photodegradation of RB 5 dye. Thus AC-CdO-TiO₂ exhibited very superior photocatalytic activity when compared to that of TiO₂, dark and nil catalyst (Figure 7). The RB 5 dye was resistant to photolysis with AC-CdO-TiO₂ nanocomposite material in the dark with a dye concentration of 1×10^{-4} M. RB 5 dye undergoes % degradation of 0, 20, 30, 62 and 98 and TiO₂ undergoes % degradation of 0, 5, 12, 30 and 59. The result indicates that AC-CdO-TiO₂ nanocomposite material has greater photocatalytic activity.

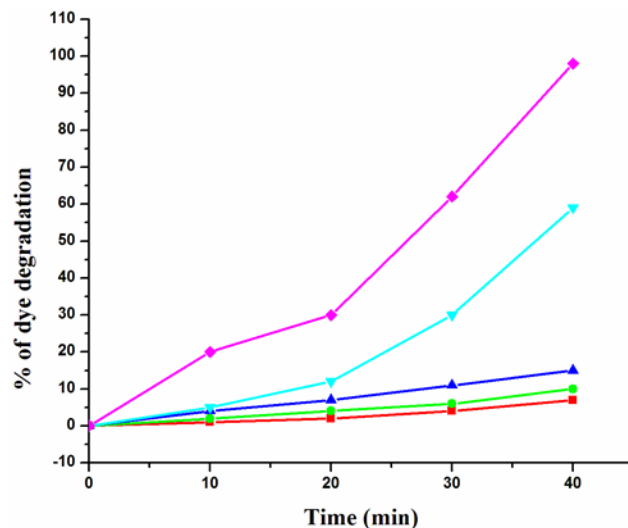


Figure 7. The effect of pH=7 photodegradation study of RB 5 dye under UV-light irradiation at 365 nm by (a) Dark (b) Nil catalyst (c) TiO₂ P25 (d) TiO₂ and (e) AC-CdO-TiO₂ nanocomposite material.

Effect of catalyst loading: Experiments performed with different amounts of AC-CdO-TiO₂ nanocomposite material showed that the photodegradation efficiency increased with an increase in amount up to 0.08 g/50 ml and then slightly decreased as observed in catalyst loadings of 0.05, 0.08 and 0.1 g/50 ml. AC-CdO-TiO₂ on RB 5 dye undergoes % of degradation 38, 98 and 60% (Figure 8). Among the catalyst loadings 0.08 g showed optimal photocatalytic activity.

Effect of different concentrations of RB 5 dye: The effect of dye concentration for the photodegradation of RB 5 dye on AC-CdO-TiO₂ nanocomposite material at 1×10^{-4} M concentration showed high photocatalytic activity than at 2×10^{-4} M and 3×10^{-4} M concentration (Figure 9). The result shows, high concentration of dye molecule decreases degradation range and catalyst surface area. So high concentration showed slow photocatalytic activity whereas low concentration of dye molecules showed fast activity of dye.

Effect of different temperature: The photodegradation of AC-CdO-TiO₂ nanocomposite material uses different calcination temperatures (200°C (18%), 400°C (50%) and 5000°C (98%)) under UV-light absorption at time 60 min. High calcination temperature showed optimum photocatalytic activity than low calcination temperature. High activity was shown corresponding to its polycrystalline nature (Figure 10).

Stability of the reusable photo catalyst: The reusability of AC-CdO-TiO₂ nanocomposite material was investigated by the

photocatalytic degradation properties of the photocatalyst by repeating RB 5 dye photocatalytic degradation experiments five times. After each cycle, the photocatalysts were washed thoroughly with water, and a fresh solution of RB 5 dye was made before each photocatalytic run in the photoreactor under UV-light and the results are shown in Figure 11.

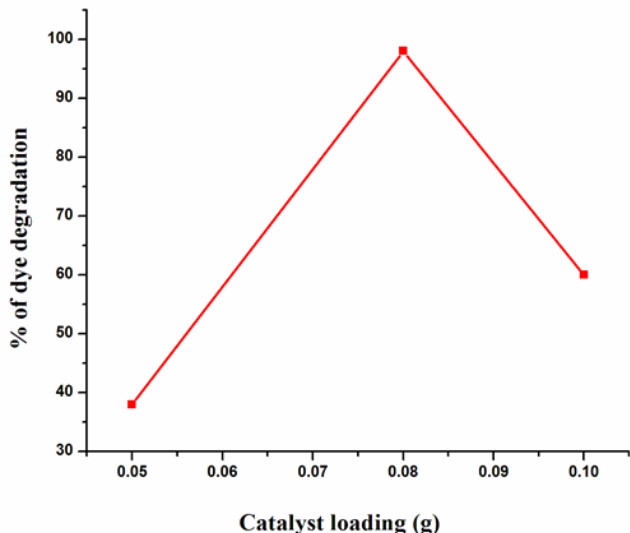


Figure 8. The effects of catalyst loading (a) AC-CdO-TiO₂ nanocomposite material on RB 5 dye under UV-light irradiation at 365 nm.

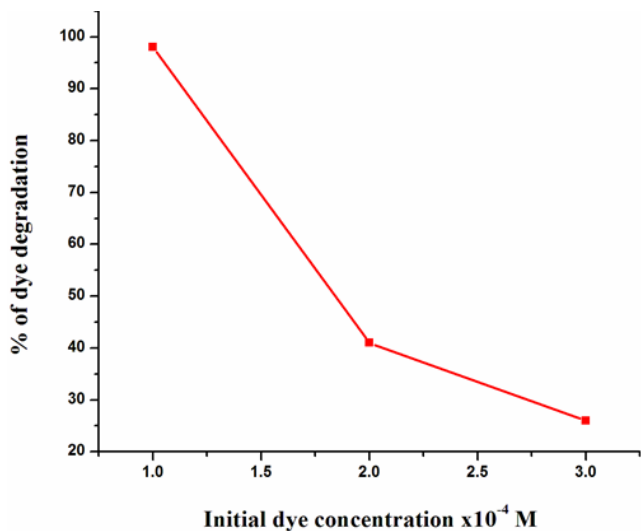


Figure 9. The effects of concentrations of (a) AC-CdO-TiO₂ nanocomposite material.

The complete degradation of the AC-CdO-TiO₂ nanocomposite material occurred in 1st-5th cycles with 97% degradation. After the fifth cycle, the efficiency of catalysts decreased in comparison to the total degradation of RB 5 dye. There is no significant change in reaction, indicating the stability of photocatalyst. This is due to the loss of catalysts (0.3%), during the water washing of catalysts, which was not observed in the naked eye in this nanocomposite material (Figure 12).

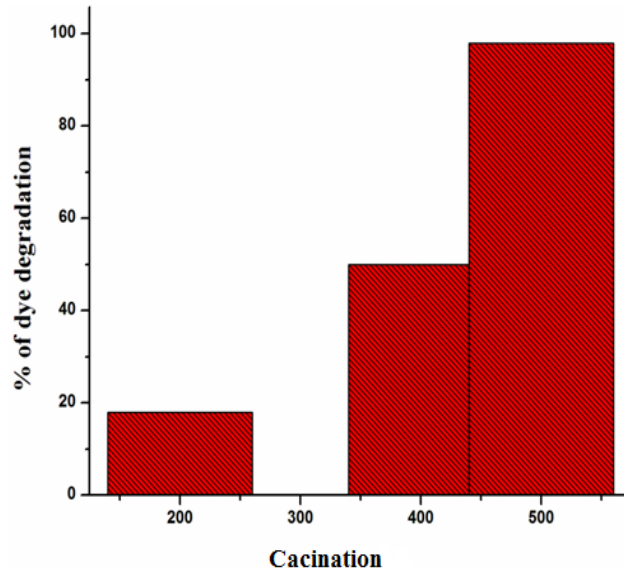


Figure 10. The effects of temperature of (a) AC-CdO-TiO₂ nanocomposite material.

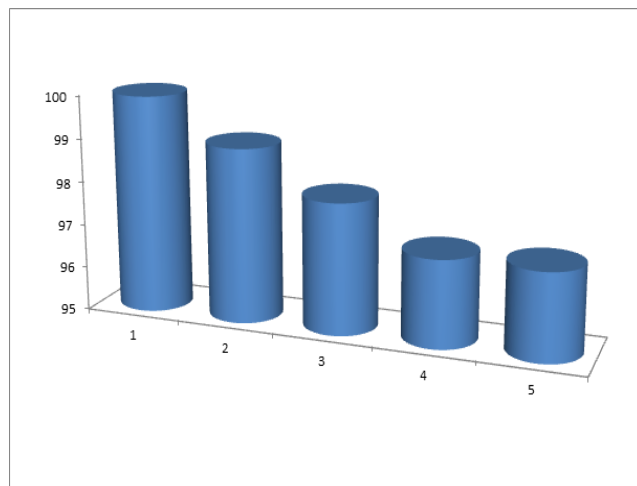
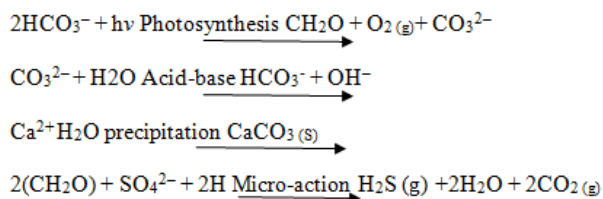


Figure 11. Stability and reusability on RB 5 dye degradation; (a) AC-CdO-TiO₂ nanocomposite material.

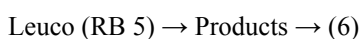
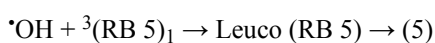
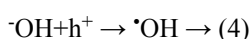
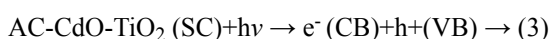
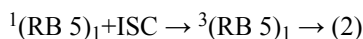
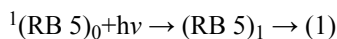
Chemical oxygen demand analysis (COD): Chemical oxygen demand analysis of RB 5 dye on mineralization of AC-CdO-TiO₂ nanocomposite material photocatalyst, loading amount of 0.080 g on dye concentration (1 × 10⁻⁴ M) suspension in 40 ml of pH=7 solution and air passing with UV-light at 365 nm (Figure 13).

AC-CdO-TiO₂ nanocomposite % of chemical oxygen demand reduction of dye at 10 min (20%), 20 min (29%), 30 min (61%) and 40 min (98%) is obtained [29].

The mineralization is also specific by formation of calcium carbonate when the evolved gas (carbondioxide) through photodegradation is accepted and calcium hydroxide is obtained. This result indicates almost complete photodegradation of dye and this reaction is as follows:



Mechanism for photocatalytic effect of AC-CdO-TiO₂: On the basis of these observations, a tentative mechanism for photocatalytic degradation of RB 5 dye is proposed as follows:



(RB 5) dye absorbs radiation of desired wavelength and it forms excited singlet state. Further, it undergoes intersystem crossing (ISC) to give its more stable triplet state. Along with this, the AC-CdO-TiO₂ nanocomposite material (SC) also utilizes this energy to excite its electron from valence band to the conduction band. An electron can be abstracted from hydroxyl ion by hole (h⁺) present in the valence band of semiconductor generating [•]OH radical. This hydroxyl radical will oxidize methyl green to its leuco form, which may be ultimately degraded to products. It was confirmed that the [•]OH radical participates as an active oxidizing species in the degradation of RB 5 dye as the rate of degradation was appreciably reduced in presence of hydroxyl radical scavenger (2-propanol) (Figure 12) [30].

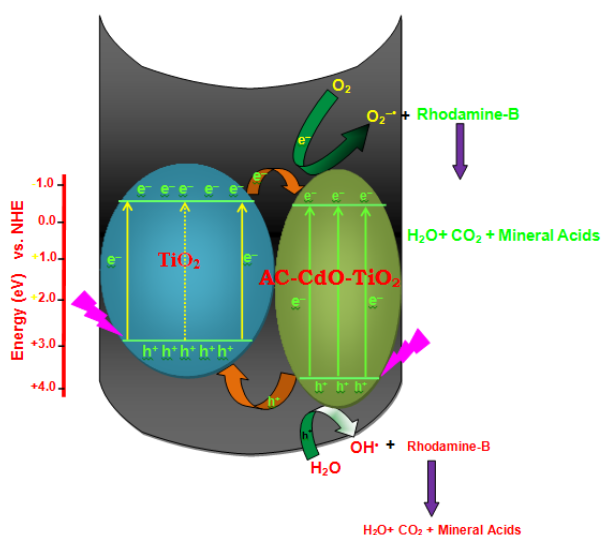


Figure 12. Degradation mechanism. Schematic representation for the photodegradation holes and electrons in the AC-CdO-SnO₂ nanocomposite material under UV-light for successive mineralization of RB 5 dye.

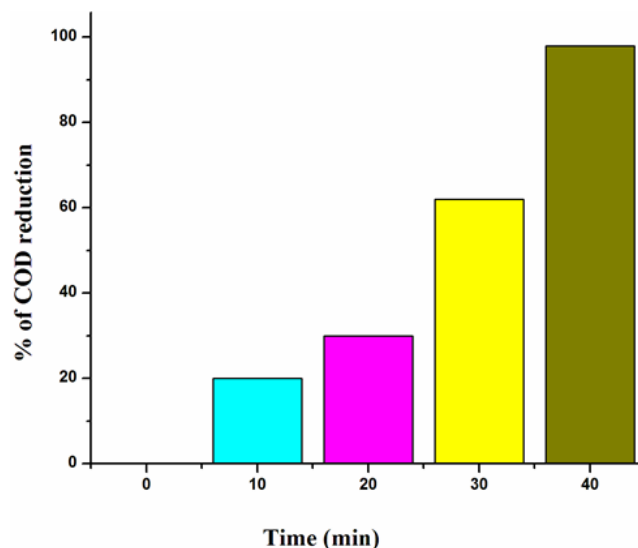


Figure 13. COD analysis of AC-CdO-TiO₂ nanocomposite material.

[•]OH analysis: The detection of [•]OH by the changes in the fluorescence spectra of a coumarin solution under visible-light irradiation as a function of irradiation time 40 min. Fluorescence intensity arises due to hydroxyl radicals as the active species. Further the formed hydroxyl radicals on the surface of AC-CdO-TiO₂ nanocomposite material illuminated by visible-light were detected by fluorescence technique same as that of TiO₂ nanocomposite material. The formation of [•]OH is directly related to the photocatalytic mechanism of the AC-CdO-TiO₂ nanocomposite material (Figure 14) [31].

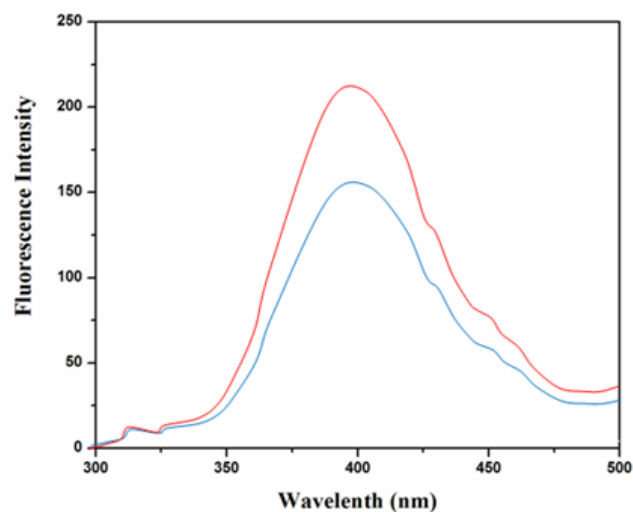


Figure 14. Fluorescence spectra measured at $\lambda_{\text{max}}=310$ nm (a) TiO₂ and (b) AC-CdO-TiO₂ nanocomposite material obtained using various time 40 min in coumarin solution (sample was illuminated for 40 min with UV light).

Electrochemical application

Cyclic voltammogram (CV) analysis: Cyclic voltammogram (CV) of methanol was recorded in alkaline medium (0.5 M NaOH) on glassy carbon electrode (GCE) and coating of catalysts in TiO₂ and AC-CdO-TiO₂ nanocomposite material

was done. The forward peak current density for methanol oxidation on AC-CdO-TiO₂ nanocomposite material showed higher electrocatalytic activity (2.5 mA cm⁻²) than TiO₂ (1 mA cm⁻²) indicating that AC-CdO-TiO₂ nanocomposite material is superior to TiO₂ (Figures 15a and 15b).

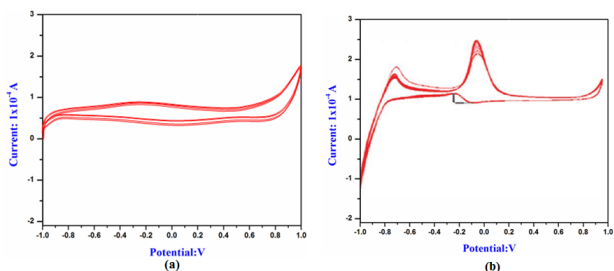


Figure 15. CV analysis of (a) TiO₂ and (b) AC-CdO-TiO₂ nanocomposite material GCE in 0.1 M KCl.

Photovoltaic properties: Figure 16 shows the photo current voltage (I-V) behavior of fabrication in the dye sensitized solar cell (DSSCs). Prepared TiO₂ and AC-CdO-TiO₂ nanocomposite material act as photoelectrode coated on fluorine doped Tin oxide (FTO-plate) glass substrate. The routine solar cell is fabricated with prepared TiO₂ and AC-CdO-TiO₂ nanocomposite material with ruthenium dye (535-bisTBA, N719). From the data, it is clear that (N719) AC-CdO-TiO₂ nanocomposite material based cell gives brilliant activity with the use of dye since the sensitizer reunites the maximum value of short-circuit current density, J_{sc} (4.9 mA/cm²) than TiO₂ (4 mA/cm²), open-circuit voltage, Voc (500 mV), fill-factor, FF (0.94) and efficiency, η (1.7%). The result indicating AC-CdO-TiO₂ nanocomposite material superior electrocatalytic activity [32,33].

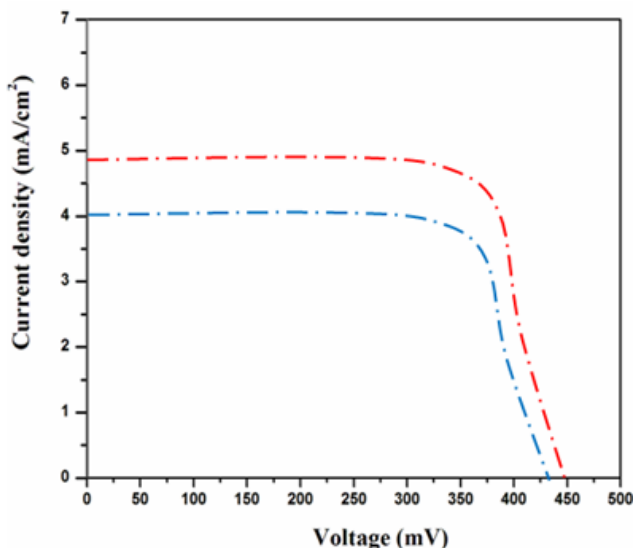


Figure 16. Current density-voltage (I-V) curves for the DSSC's fabricated from (a) TiO₂ coated GCE in 0.1 M KCl and (b) AC-CdO-TiO₂ nanocomposite material GCE in 0.1 M KCl.

Conductivity studies: Photoconductivity result of AC-CdO-TiO₂ nanocomposite material represent increased current and increased charge carriers in photocurrent compared to dark

current. This nanocomposite material exhibited (+ve) photoconductivity as well as solar cell application (Figure 17) [34,35].

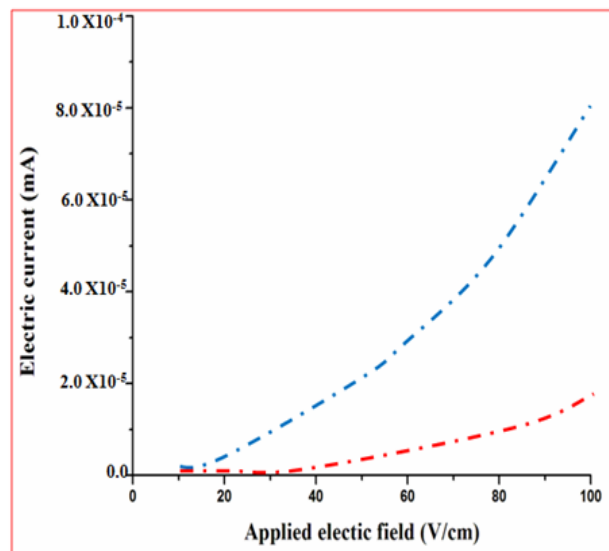


Figure 17. Photoconductivity of AC-CdO-TiO₂ nanocomposite material. Applied field (V cm⁻¹) vs. electric current (mA) (a) dark and (b) photocurrent on irradiation with 100 W halogen lamp.

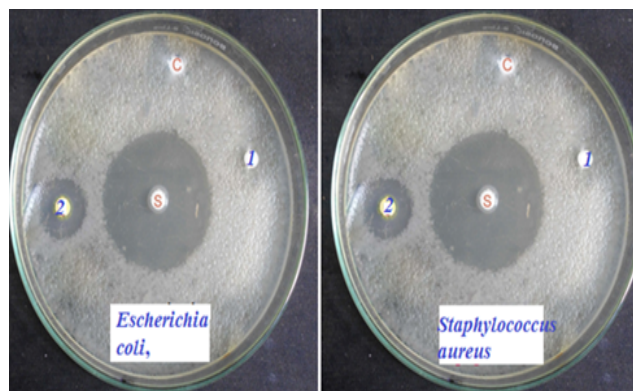


Figure 18. Antibacterial activity (disc diffusion method) (1) of TiO₂ nanomaterial and (2) of AC-CdO-TiO₂ nanocomposite material on (a) *Escherichia coli* (b) *Staphylococcus aureus*

Antibacterial activity

Antibacterial activity of TiO₂ and AC-CdO-TiO₂ nanocomposite material are shown in Figure 18. CdO-SnO₂ nanocomposite material showed activity against both Gram positive strains and Gram negative strains. 15 mm and 11 mm inhibition zone was developed against *Escherichia coli* and *Staphylococcus aureus*. The AC-CdO-TiO₂ nanocomposite material showed high antibacterial activity against Gram positive bacteria rather than Gram negative bacteria. This was due to the differences in the cell wall composition of these two bacteria. AC-CdO-TiO₂ nanocomposite material increases the value of the electron-holes charge separation by decreasing the band gap energy which leads to an impediment in the recombination rate for high antibacterial activity, hence used in biomedical applications [36,37].

Conclusion

The mild reaction conditions, easy work-up, clean reaction profiles render this approach as an interesting alternative to the existing methods. The HR-SEM image of AC-CdO-TiO₂ nanocomposite material showed the morphological structure as nanoflakes which were further confirmed by EDX analysis. HR-TEM measurements indicated nanospherical chain shaped structures corresponding to its polycrystalline nature. The photodegradation efficiency of AC-CdO-TiO₂ nanocomposite material on RB 5 showed a high photocatalytic activity by employing various experimental parameters namely high photocatalytic effect of pH=7 whereas the nanocomposite material with the catalyst (0.080 g) loading showed optimum photocatalytic activity when compared to TiO₂, furthermore, nanocomposite material at concentration of 1×10^{-4} M showed high photocatalytic activity with the catalysis was stable and recyclable. Finally, AC-CdO-TiO₂ nanocomposite material was found to show high antibacterial activity on (a) *Escherichia coli*, (b) *Staphylococcus aureus* and a high current produced effective short circuit than that of TiO₂ nanocomposite material.

Conflict of Interest

The authors declare no competing financial interest.

References

- Balakrishnan M, Arul Antony S, Gunasekaran S, Natarajan RK. Impact of dyeing industrial effluents on the groundwater quality in Kancheepuram (India). *Ind J Sci Technol* 2008; 1: 1.
- Vijaykumar MH, Vaishampayan PA, Shouche YS, Karegoudar TB. Decolouri-zation of naphthalene-containing sulfonated azo dyes by *Kerstersia* sp strain VKY1. *Enzym Microb Tech* 2007; 204-211.
- Asad S, Amoozegar MA, Pourbabaee AA, Sarbolouki MN, Dastgheib SM. Decolorization of textile azo dyes by newly isolated halophilic and halotolerant bacteria. *Bioresour Technol* 2007; 98: 2082-2088.
- Liu W, Chao Y, Yang X, Bao H, Qian S. Biodecolorization of azo, anthraquinonic and triphenylmethane dyes by white-rot fungi and a laccase-secreting engineered strain. *J Ind Microbiol Biotechnol* 2004; 31: 127-132.
- OMahony T, Guibal E, Tobin JM. Reactive dye biosorption by *Rhizopus arrhizus* biomass. *Enzym Microb Tech* 2002; 31: 456-463.
- Balachandran S, Praveen SG, Velmurugan R, Swaminathan M. Facile fabrication of highly efficient, reusable heterostructured Ag-ZnO-CdO and its twin applications of dye degradation under natural sunlight and self-cleaning. *RSC Adv* 2014; 4: 4353-4362.
- Kalele S, Gosavi SW, Urban J, Kulkarni SK. Nanoshell particles: synthesis, properties and applications. *Curr Sci* 2006; 91: 1038-1052.
- Manikandan A, Judith Vijaya J, John Kennedy L. Comparative investigation of structural, optical properties and dyesensitized solar cell applications of ZnO nanostructures. *J Nanosci Nanotechnol* 2013; 13: 3068-3073.
- Loganathan B, Chandraboss VL, Murugavelu M, Senthilvelan S, Karthikeyan B. Synthesis and characterization of multimetallic-core and siliceousshell Au/Pt/Ag@SiO₂ sol-gel derived nanocomposites. *J Sol-Gel Sci Tech* 2014.
- Murugavelu M, Karthikeyan B. Synthesis, characterization and evaluation of green catalytic activity of nano Ag-Pt doped silicate. *J Alloys Comp* 2013; 547: 68-75.
- Shon HK, Phuntsho S, Vigneswaran S. A study on the influence of ionic strength on the elution behaviour of membrane organic foulant using advanced separation tools. *Desaline Water Treat* 2008; 225: 235-248.
- Yiamsawas D, Boonpavanitchakul K, Kangwansupamonkon W. Preparation of ZnO nanostructures by solvothermal method. *Microsc J Soc Thailan* 2009; 23: 75-78.
- Balachandran S, Prakash N, Thirumalai K, Muruganandham M, Sillanpaa M, Swaminathan M. Facile construction of heterostructured BiVO₄-ZnO and its dual application of greater solar photocatalytic activity and self-cleaning property. *Ind Eng Chem Res* 2014; 53: 8346-8356.
- Balachandran S, Swaminathan M. The simple, template free synthesis of a Bi₂S₃-ZnO heterostructure and its superior photocatalytic activity under UV-A light. *Dalton Trans* 2013; 42: 5338-5347.
- Papp J, Soled S, Dwight K, Wold A. Surface acidity and photocatalytic activity of TiO₂, WO₃/TiO₂, and MoO₃/TiO₂ photocatalysts. *Chem Mater* 1994; 6: 496-500.
- Fu X, Clark LA, Yang Q, Anderson MA. Enhanced photocatalytic performance of titania-based binary metal oxides: TiO₂/ SiO₂ and TiO₂/ZrO₂. *Environ Sci Technol* 1996; 30: 647-653.
- Chanchal M, Mainak G, Arun KS, Jaya P, Ramkrishna S, Tarasankar P. Robust cubooctahedron Zn₃V₂O₈ in gram quantity: a material for photocatalytic dye degradation in water. *Cryst Eng Comm* 2013; 15: 6745-6751.
- Tanmay KG, Niladri B. Photodegradation of rhodamine 6G in aqueous solution via SrCrO₄ and TiO₂ nano-sphere mixed oxides *J Mater Res Technol* 2013; 2: 10-17.
- Rui S, Yajun W, Feng Z, Yongf Z. Zn₃V₂O₇(OH)₂(H₂O)₂ and Zn₃V₂O₈ nanostructures: controlled fabrication and photocatalytic performance. *J Mater Chem* 2011; 21: 6313.
- Kamalakkannan J, Chandraboss VL, Prabha S, Senthilvelan S. Advanced construction of heterostructured InCrO₄-TiO₂ and its dual properties of greater UV-photocatalytic and antibacterial activity. *RSC Adv* 2015; 5: 77000-77013.

21. Kamalakkannan J, Chandraboss VL, Loganathan B, Prabha S, Karthikeyan B, Senthilvelan S. TiInCrO₆-nanomaterial synthesis, characterization and multiapplications. *Appl Nanosci* 2015.
22. Kamalakkannan J, Chandraboss VL, Prabha S, Karthikeyan B, Senthilvelan S. High photocatalytic activity of heterostructured InMoO₃-TiO₂ nanocomposite material under natural sun light irradiation. *Can Chem Trans* 2015; 3: 327-339.
23. Tsumura T, Kojitani N, Umemura H, Toyoda M, Inagaki M. Composites between photoactive anatase-type TiO₂ and adsorptive carbon. *Appl Surf Sci* 2002; 196: 429-436.
24. Velasco LF, Parra JB, Ania CO. Role of activated carbon features on the photocatalytic degradation of phenol. *Appl Surf Sci* 2010; 256: 5254-5258.
25. Mezohegyi G, van der Zee FP, Font J, Fortuny A, Fabregat A. Towards advanced aqueous dye removal processes: a short review on the versatile role of activated carbon. *J Environ Manage* 2012; 102: 148-164.
26. Kamalakkannan J, Chandraboss VL, Prabha S, Senthilvelan S. Activated carbon loaded N, S co-doped TiO₂ nanomaterial and its dye wastewater treatment. *Inter Lett Chem Phy Astron* 2015; 8: 147-164.
27. Prabha S, Chandraboss VL, Kamalakkannan J, Senthilvelan S. UV-light assisted photodegradation and antibacterial activity of activated charcoal supported cadmium doped ZnO nanocomposite material. *Inter J Modern Res Rev* 2015; 3: 587-594.
28. Chandraboss VL, Kamalakkannan J, Senthilvelan S. Characterization of activated charcoal supported bismuth doped SiO₂ (ac-Bi@SiO₂) nanocomposite sphere for photocatalytic application. *Can Chem Trans* 2015; 3: 410-429.
29. Subash B, Krishnakumar B, Swaminathan M, Shanthi M. Highly efficient, solar active, and reusable photocatalyst: Zr-loaded Ag-ZnO for reactive red 120 dye degradation with synergistic effect and dye-sensitized mechanism. *Langmuir* 2013; 29: 939-949.
30. Kamalakkannan J, Senthilvelan S. Morphology convenient flower like nanostructures of CdO-SiO₂ nanomaterial and its photocatalytic application. *WSN* 2017; 62: 46-63.
31. Chandraboss VL, Kamalakkannan J, Prabha S, Senthilvelan S. An efficient removal of methyl violet from aqueous solution by an AC-Bi/ZnO nanocomposite material. *RSC Adv* 2015; 5: 25857-25869.
32. Zhang Y, Wang L, Liu B, Zhai J, Fan H, Wang D, Lin Y, Xie T. Synthesis of Zn-doped TiO₂ microspheres with enhanced photovoltaic performance and application for dye-sensitized solar cells. *Electrochimica Acta* 2011; 56: 6517-6523.
33. Kamalakkannan J, Chandraboss VL, Prabha S, Karthikeyan B, Senthilvelan S. Preparation and characterization of TiInVO₆-nanomaterial using precipitation method and its multi applications. *J Mater Sci Mater Electron* 2015.
34. Balachandran S, Selvam K, Babub B, Swaminathan M. The simple hydrothermal synthesis of Ag-ZnO SnO₂nanochain and its multiple application. *Dalton Trans* 2013; 42: 16365-16374.
35. Balachandran S, Thirumalai K, Swaminathan M. Facile hydrothermal synthesis of a highly efficient solar active Pr₆O₁₁-ZnO photocatalyst and its multiple applications. *RSC Adv* 2014; 1-12.
36. Banerjee S, Gopal J, Muraleedharan P, Tyagi AK, Raj B. Physical and chemistry of photocatalytic titanium dioxide visualization of bactericidal activity using atomic force microscopy. *Curr Sci* 2006; 90: 1378-1383.
37. Kiran G, Singh RP, Ashutosh P, Anjana P. Photocatalytic antibacterial performance of TiO₂ and Ag- doped TiO₂ against *S. aureus*, *P. aeruginosa* and *E. coli*. *Beilstein J Nanotechnol* 2013; 4: 345-351.

***Correspondence to**

Marimuthu G

Department of Chemistry

Swami Dayananda College of Arts and Science

Tamil Nadu

India